

Nanostructured carbon films from supersonic cluster beam deposition: structure and morphology

P. Milani^{1,a}, E. Barborini¹, P. Piseri¹, C.E. Bottani², A.C. Ferrari^{2,b}, and A. Li Bassi²

¹INFM-Dipartimento di Fisica, Università di Milano, Via Celoria 16, I-20133 Milano, Italy

²INFM-CESNEF, Politecnico di Milano, Via Ponzio 34/3, I-20133 Milano, Italy

Received: 1 September 1998 / Received in final form: 28 September 1998

Abstract. Nanostructured carbon thin films have been grown by deposition of cluster beams produced by a supersonic expansion. Due to separation effects typical of supersonic beams, films with different nanostructures can be grown by the simple intercepting of different regions of the cluster beam with a substrate. Films show a low-density porous structure, which has been characterized by Raman and Brillouin spectroscopy. Film morphology suggests that growth processes are similar to those occurring in a ballistic deposition regime.

PACS. 81.15.Hi Molecular, atomic, ion, and chemical beam epitaxy – 81.05.Tp Fullerenes and related materials; diamonds, graphite – 81.05.Ys Nanophase materials

1 Introduction

The physico-chemical properties of carbon thin films are influenced by a series of features, i.e., the coexistence of different atomic coordination, the degree of crystallinity, texture, voids, surface roughness, etc. High-density sp^3 films show outstanding mechanical properties [1]. On the other hand, sp^2 films with high roughness and porosity are interesting for catalysis and electrochemistry [2]. Film morphology and structure are determined by growth processes, where critical lengths range from nanometer up to micrometer scales. The understanding and control of these processes could help one in finding new synthetic routes and in making progress towards a unified description of the astonishingly large variety of carbon allotropes and carbon-based solids.

Different synthetic strategies are adopted, depending on which properties one wants to enhance in the film. Atom-by-atom growth is used for the production of high-density films with good mechanical properties and small surface roughness [3], whereas chemical routes based on polymeric precursors are used to produce porous forms of carbons [2]. These latter techniques are not particularly suitable for the production of thin films.

The use of carbon clusters as building blocks for carbon films has opened up new perspectives for the synthesis of films with improved mechanical properties [4]. On the other hand, it has been shown that low-energy car-

bon cluster beam deposition can be used for the synthesis of nanostructured films characterized by a low-density structure reminiscent of the precursor clusters [5, 6]. This new material, which we can call nanostructured carbon (ns-C), shows properties interesting for electronic applications, such as field emission devices [7].

A systematic characterization of the structural and functional properties of ns-C is only the beginning, and in particular the influence of the cluster mass distribution and structure on the final properties of the film is still to be investigated. To accomplish this task, it is very important to have a well-characterized cluster beam and to use characterization techniques sensitive to different length scales in order to discriminate between different contributions coming from different atomic coordinations, single-cluster structures and cluster-cluster interactions.

Here we will show that the use of supersonic beams provide unique opportunities for ns-C film deposition in terms of deposition rates and the control of cluster size distributions. We report here a characterization of the structural and mechanical properties of ns-C showing that the films retain a memory of the precursor clusters. The morphology of the films is also reminiscent of the low-energy deposition regime. Features observed on a mesoscopic scale suggest a ballistic deposition regime of growth.

2 Experimental setup

The experimental apparatus for nanostructured thin film deposition consists of three differentially evacuated chambers and operates in the high vacuum regime. The first

^a e-mail: pmilani@mi.infn.it

^b Present address: Department of Engineering, Cambridge University, Cambridge, UK

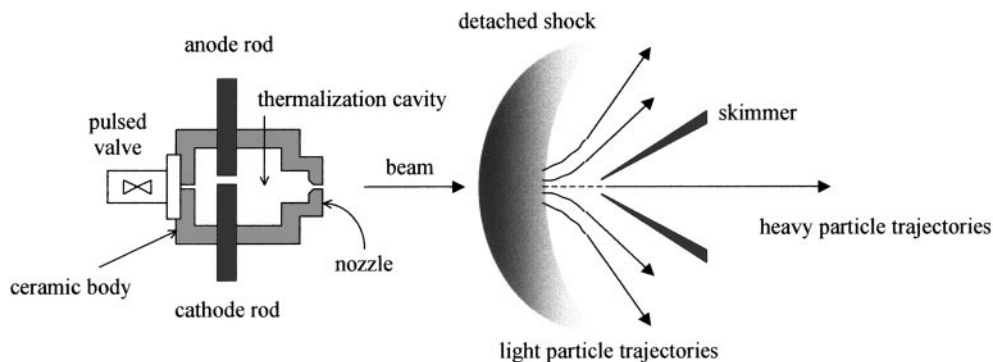


Fig. 1. Schematic representation of the pulsed cluster source placed in front of the skimmer of the first chamber. By properly adjusting the source-skimmer distance and the chamber background pressure, a detached shock is produced. Because of their lower inertia, light particles are diverted from the center beam, while the heavy ones follow straight-line trajectories.

one, a \varnothing 250 mm stainless steel cylindrical vessel, hosts the cluster source and is evacuated by a 2000 l/s oil diffusion pump in order that an average pressure in the range of $1\text{--}3 \times 10^{-5}$ torr may be maintained, despite the high gas load necessary for optimum source operation. Base pressure in the source chamber is typically 1×10^{-7} torr. The second chamber is equipped with a sample holder which can intersect with the supersonic beam and a quartz microbalance for beam intensity monitoring; it can alternatively host a beam-chopper and a fast ionization gauge for time-of-flight measurements of the velocity distribution of particles in the beam. The deposition chamber is evacuated by an oil diffusion pump at a background pressure of typically 1×10^{-7} torr. The third chamber hosts a Time-Of-Flight Mass Spectrometer (TOF/MS). The TOF/MS is a short linear one performing second-order space focusing [8], and is placed collinear to the beam axis in order that the best transmission on the full mass range covered by the electron multiplier ion detector [9] may be achieved. The detector of the TOF/MS, being sensitive to high-speed neutral clusters as well, can also be used in conjunction with a beam chopper for time of flight characterization [10].

Our cluster source is a modified version of the PACIS source [11], and it works vaporizing the material used for cluster production with a pulsed electrical discharge. A schematic cross section of the source is sketched in Fig. 1. Two electrodes of the material to be vaporized (graphite in this case) face each other in a small cavity inside the ceramic body of the source. A pulsed valve injects some inert gas inside the cavity so that an electrical discharge can take place between the two electrodes. The discharge, driven by high voltage (between 500 and 1500 V), is very intense (~ 1000 A), lasting a few tens of microseconds, and produces the ablation of the cathodic material. This is quenched by inert gas and condenses in clusters, which are carried out of the source in a seeded supersonic expansion [12]. With a proper design of the source nozzle, high-intensity, well-collimated cluster beams can be produced, and deposition rates up to 5 nm/s on the beam axis can be obtained. Moreover, if the nozzle-skimmer or interference is exploited to produce separation effects (Fig. 1), films with different mass distribu-

tion of the precursor clusters can be deposited (see below) [13].

From a schematic point of view, we can say that our source has many characteristics typical of gas aggregation sources, and that, because of this, it is intense and stable. On the other hand, it can produce a pulsed supersonic beam which is particularly attractive for thin film deposition.

3 Cluster beam characterization, manipulation and film deposition

With typical discharge conditions, we obtain a log-normal cluster mass distribution in the range of 0 – 1500 atoms/clusters, with a maximum peaked at around 400 atoms/cluster and an average size at about 950 atoms/cluster.

During operation, the source body reaches a temperature of ≈ 400 K. Stagnation temperature of the carrier gas is, however, a function of time, evolving very rapidly down to ≈ 100 K as expansion takes place and the source gets empty. The velocity of the carrier gas is thus about 2000 m/s at the time the first clusters come out of the nozzle, but slows down to ≈ 1000 m/s at the tail of the cluster pulse. A velocity slip of the clusters with respect to the carrier gas is also present but becomes of some relevance only for clusters exiting late from the source, when the stagnation pressure is reduced.

From these time of flight measurements, we see that the kinetic energy of the clusters is lower than 0.2 eV/Atom, well below the binding energy of carbons in the cluster. At cluster impact on the surface, there is thus no substantial fragmentation of the aggregates, and deposited films may keep memory of the structure the clusters had in the gas phase [6].

Several approaches have been proposed for controlling the cluster mass distribution. The local pressure where the target vaporization takes place and the residence time of the clusters in the source strongly affect the cluster size distribution. Unfortunately, a change of these parameters often corresponds to an instability of the source. In gas aggregation sources and in particular for pulsed sources with

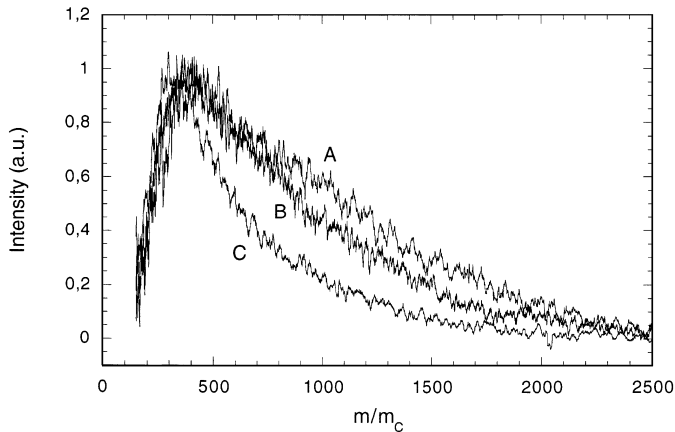


Fig. 2. Cluster mass distributions obtained from a pulsed plasma source with different nozzle diameters. The distributions are obtained by the averaging for all different residence times of the clusters inside the source.

aggregation chambers, the residence time can be varied if the nozzle diameter, and thus the time necessary for emptying the source, is changed. Cluster mass distributions produced with our source with different nozzle diameters are shown in Fig. 2. The center of the mass distribution moves toward higher masses when the nozzle diameter is reduced. This can be explained by the fact that clusters experience a longer residence time, hence there are more collisions inside the aggregation chamber. The use of different nozzles does not allow a fine control over the mass distribution, and in our case, only an enrichment of very large clusters is observed. A possible way to circumvent this problem is a radical change in source dimensions, but this will work only for the production of large clusters [14]. The conditions for the production of small clusters are at odds with high intensities and stability.

Cluster separation can be also obtained in the beam. Usually this method is applied on charged clusters using electromagnetic selectors, such as quadrupoles or Wien filters [15, 16]. Although beams that are monochromatic in mass can be obtained, the beam intensity is so low that their use for thin film deposition is impractical.

By taking advantage of the separation effects attainable in supersonic expansions, the mass distribution of neutral clusters can be efficiently controlled. Since the pioneering work on supersonic jets [17, 18], it has been recognized that if species with different weights are present in the gas to be expanded, the heavier constituents become concentrated along the core of the beam. Different mechanisms have been proposed to account for these effects. Reis and Fenn [17] have shown that one can obtain mass separation by exploiting the interaction of the beam with the shock wave detached from the skimmer (see Fig. 1). In particular, because of the species' different inertia, the light species follow diverging streamlines after the shock front, whereas the heavy species are not diverted, and can follow straight trajectories through the skimmer. Because of this effect, large clusters are concentrated in the central portion of the beam, whereas the lighter ones are at the periphery.

In our apparatus, due to the long gas pulse exiting from the source with a condensation cavity, (i.e., the high duty cycle of the source), the source-skimmer distance D_{sk} and the gas pressure in the first chamber are important parameters to be controlled. Depending upon D_{sk} , a shock wave can be produced in front of the skimmer, causing mass separation effects and affecting the final characteristics of the beam.

Selecting a portion of the beam with a skimmer, circular films with a radius of 1 cm and uniform thickness can be deposited in the second chamber of the apparatus. Intersecting the beam in the first chamber films with an area of several cm^2 , one can prepare a film with a thickness which is uniform on a scale considerably larger than that of the experimental probes used for characterization.

In analogy with aerosol apparatus, where inertial effects are used for separation of particles [19], we have used separation effects to deposit thin films by intersecting different regions of the beam spot with a substrate (Fig. 1). Since clusters maintain, at least partially, their original structure [5, 13], the films should be reminiscent of the precursor clusters and present different coordinations and local order.

4 Film growth and morphology

It is well known that the morphology of thin films show, regardless of the material, universal characteristics [20]. These ubiquitous features, consisting of arrays of columnar and conical structures, are correlated with low adatom mobility. Since deposition is usually performed on substrates kept at temperatures considerably lower than the melting point of the deposited material, a regime where the impinging particles have a low mobility is common.

The general occurrence of morphological similarities, not only between different materials but also on different length scales, as the growth takes place, suggests that a nonspecific mechanism is responsible for the observed morphologies, and that formation, growth, and dynamics of film surfaces can be described in terms of scaling relations and universality classes [20]. Different growth mechanisms have been proposed, such as random and ballistic deposition, the critical ingredient for all the models being surface diffusion.

Cluster beam deposition allows one to investigate how the precursor particle dimensions affect thin film morphologies and, more generally, whether there is any influence of the particle dimensions on the scaling parameters.

The film growth mechanisms with cluster beam deposition has been studied for the very initial stages at submonolayer coverages [21, 22]. No systematic characterization of the further stages of growth have been undertaken so far. The evolution of film structure and of film surface roughness is of particular interest for thick films, since these parameters evolve with thickness in a way that is not yet clear.

In Fig. 3, the surface, and a section of cluster-assembled carbon films are shown. In Fig. 3a, the surface of a thin

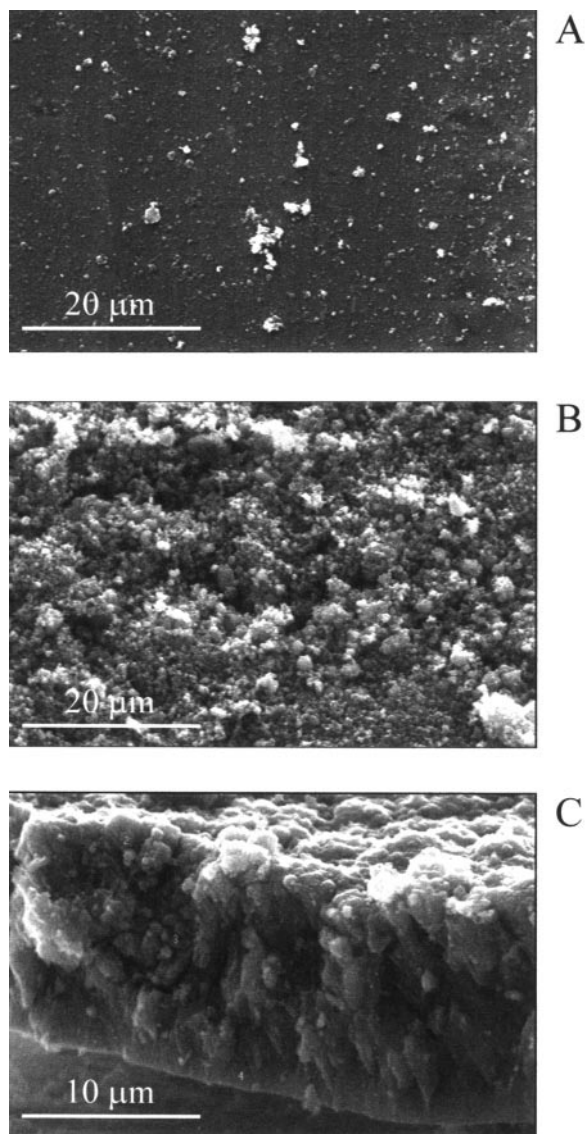


Fig. 3. SEM micrographs of the surface and of the section of ns-C films. (a) Surface of a film with $\leq 1 \mu\text{m}$ thickness. (b) Surface of a $15 \mu\text{m}$ thick film. (c) Section of a thick film showing conical and nodular structures. Different morphologies observed with this scale of magnification are due to different film thicknesses.

film ($\leq 1 \mu\text{m}$) is fairly flat at this scale of magnification, whereas, at the same scale, a film $15 \mu\text{m}$ thick shows a disordered and highly corrugated structure (Fig. 3b). The roughness evolution, characterized with scanning electron microscopy and atomic force microscopy, indicates that the surface may be self-affine. The film section reported in Fig. 3c shows conical and nodular features typical of a low-mobility deposition regime [23].

Cones and spherical nodules develop as the film grows. At higher magnification, the cones are composed by dendritic structures (not shown). The large number of these defects indicates that the mobility of the clusters is very low. However, the role of the deposition rate must also be decoupled and separately studied.

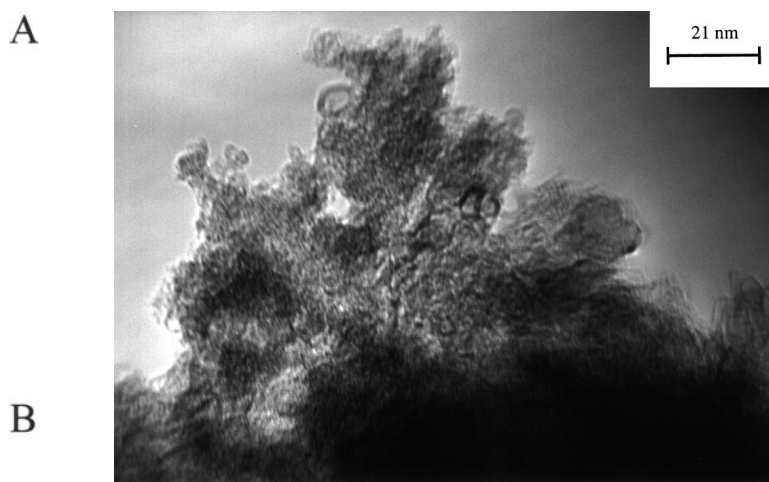


Fig. 4. TEM micrograph showing closed graphitic particles and graphene sheets dispersed among amorphous material.

5 Structural and mechanical properties

The nanostructure of an ns-C film is shown in Fig. 4. The TEM picture shows the presence of closed graphitic particles and graphene sheets in analogy to what was reported in [4].

In order to characterize the films deposited with different portions of the supersonic beam, we have performed Raman spectroscopy studies, which are sensitive to the carbon coordination and degree of crystallinity on a nanometric scale (Fig. 5). The top spectrum in Fig. 5 is taken on a region rich in small clusters (periphery of the beam). The shape and the shift of the peak (G band) are typical of a highly disordered carbon [24]. The D peak is present as a broad shoulder on the left of the G band. The peak at 2150 cm^{-1} is quite unusual for disordered carbon produced by the deposition of carbon atoms or ions, and it can be attributed to the presence of carbon chains characterized by *sp* acetylenic bonding [25].

Going from the top to the bottom spectrum in Fig. 5, one can follow the evolution from an amorphous to a disordered graphitic structure by shifting from the periphery of the beam towards the central region (large clusters). This evolution is confirmed by a hardening of the G peak, the appearance of a well-defined D band, and by the narrowing of the two Raman lines. All these parameters are in agreement with a more pronounced graphitic ordering of the sample [24].

The spectra are typical of a disordered carbon, with a high degree of *sp*² coordination. The spectral features relative to broadened and highly overlapping G and D bands suggest that the phonon density of states is different from that of graphite because of the presence of different types of disorder (bond angle and length defects, which yield different coordination with respect to graphitic *sp*²). The degree of disorder is such that even in the region with large clusters, the Tuinstra–Koenig relationship is not valid [24]. Preliminary TEM investigation suggests that the nanostructure of the film depends on the size of the precursor clusters. A correlation with

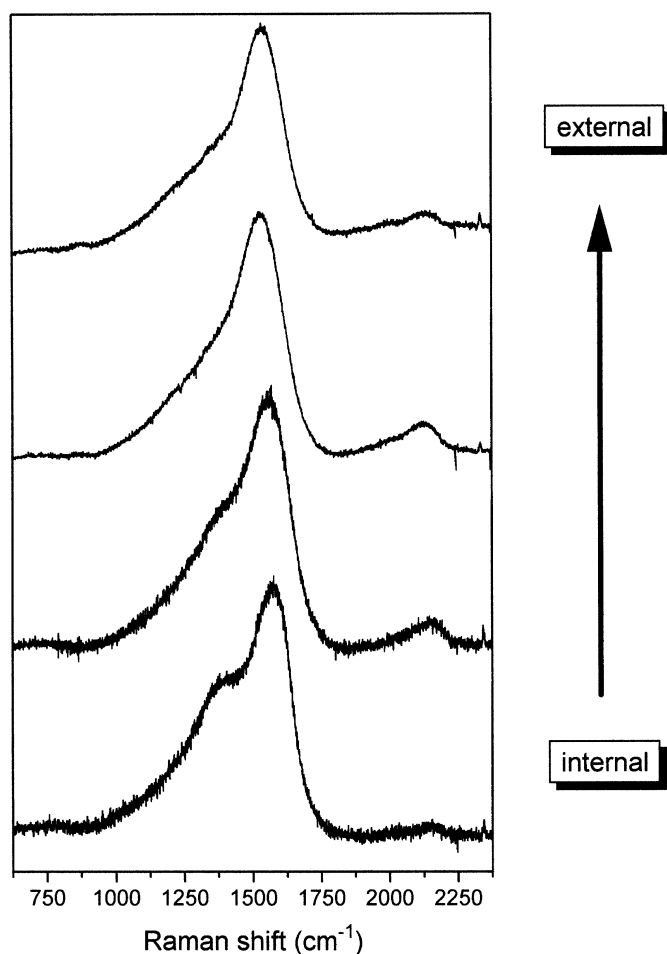


Fig. 5. First order Raman spectra of films deposited with different portions of the cluster beam. Going from the bottom (internal part of the beam i.e. large clusters) to the top spectrum (external part of the beam, i.e. small clusters) one can see the evolution from a disordered graphitic structure to an amorphous one. The peak around 2150 cm^{-1} can be related to *sp* bonds.

the trend observed with Raman spectroscopy is under investigation.

A ns-C film mass density of 1.1 g/cm^3 has been evaluated by optical ellipsometry [6] and by X-ray reflectivity measurements. The mechanical properties of this kind of soft material cannot be determined by nanoindentation methods, due to the large surface roughness related to the nanostructure of the films.

Brillouin scattering can be used to characterize the elastic properties of thin films. We have recently demonstrated that this technique can be also used in the case of rough and granular films [26]. The adiabatic effective bulk and shear moduli of cluster-assembled carbon films have been determined. The value of shear modulus, of the order of 4 GPa, compares with the C_{44} elastic constant of hexagonal crystalline graphite ($2 \approx 4\text{ GPa}$), at a length scale of several hundreds of nanometers. The bulk modulus of $\approx 3.7\text{ GPa}$ differs significantly from that of crystalline graphite ($\sim 35\text{ GPa}$).

Surface Brillouin scattering probes surface acoustic phonons with a wavelength of several hundreds of nanometers. If the surface roughness or domains have typical dimensions comparable to this value, the medium cannot be considered as a continuum for acoustic excitations, and localization phenomena can take place. One can observe this in the evolution of our film by increasing the thickness and thus the roughness. Thin films ($\leq 200\text{ nm}$) show defined surface Brillouin peaks, whereas thicker films show a broadening and a disappearance of these peaks, together with the appearance of a strong central peak.

6 Summary

The present experiments show that supersonic cluster beams are a promising tool for the synthesis of nanostructured thin films. Carbon films have been prepared by depositing high-intensity beams produced by a pulsed discharge source. Separation effects typical of supersonic beams have been used to control the cluster mass distribution in the beam and to deposit films with different nanostructures, as confirmed by Raman spectroscopy. The films are characterized by low-density and mechanical properties similar to those of a graphitic material. The morphology of the films indicates that growth processes are affected by the very low mobility of clusters after deposition. Surfaces may have a self-affine character, the dependence of surface evolution from the precursor clusters is under investigation.

Financial support from INFM Advanced Research Project CLASS is acknowledged.

References

1. J. Robertson: *Surf. Coat. Technol.* **50**, 185 (1992)
2. A.W.P. Fung, Z.H. Wang, K. Lu, M.S. Dresselhaus, R.W. Pekala: *J. Mater. Res.* **8**, 1875 (1993)
3. See, for example: *Diamond and Diamond-like Films and Coatings* ed. by R.E. Clausing, L.L. Horton, J.C. Angus, P. Koidl, NATO ASI Series B, vol. 266 (Plenum Press, New York 1991)
4. G.A.J. Amaratunga, M. Chhowalla, C.J. Kiely, I. Alexandrou, R. Aharonov, R.M. Devenish: *Nature (London)* **383**, 321 (1996)
5. A. Perez, P. Melinon, V. Dupuis, P. Jensen, B. Prevel, J. Tuaillon, L. Bardotti, C. Martet, M. Treilleux, M. Broyer, M. Pellarin, J.L. Vialle, B. Palpant, J. Lerme: *J. Phys. D: Appl. Phys.* **30**, 709 (1997)
6. P. Milani, M. Ferretti, P. Piseri, C.E. Bottani, A. Ferrari, A. Li Bassi, G. Guizzetti, M. Patrini: *J. Appl. Phys.* **82**, 5793 (1997)
7. A. Ferrari, B.S. Satyanarayana, J. Robertson, W.I. Milne, E. Barborini, P. Piseri, P. Milani: *Europhys. Lett.* **46**, 245 (1999)
8. P. Piseri, P. Milani, S. Iannotta: *Int. J. Mass Spectrom. Ion Processes*, **153**, 23 (1996)
9. U. Zimmermann, U. Naher, S. Frank, T.P. Martin, N. Malinowsky: *Large Clusters of Atoms and Molecules* ed. by

- T.P. Martin, NATO ASI Series, vol. E313 (Kluwer, Dordrecht 1996) p. 511
10. P. Piseri, A. Li Bassi, P. Milani: *Rev. Sci. Instrum.* **69**, 1647 (1998)
 11. G. Gantefoer, H.R. Siekmann, H.O. Lutz, K.H. Meiwes-Broer: *Chem. Phys. Lett.* **165**, 293 (1990)
 12. D.R. Miller: *Atomic and Molecular Beam Methods*, ed. by G. Scoles, vol. I (Oxford University Press, Oxford 1988) chap. 2
 13. E. Barborini, P. Piseri, A. Li Bassi, A. Ferrari, C.E. Bottani, P. Milani: *Chem. Phys. Lett.* **300**, 633 (1999)
 14. H. Haberland, M. Karrais, M. Mall, Y. Turner: *J. Vac. Sci. Technol. A* **10**, 3266 (1992)
 15. U. Heiz, F. Vanolli, L. Trento, W.-D. Schneider: *Rev. Sci. Instrum.* **68**, 1986 (1997)
 16. B. Wrenger, K.H. Meiwes-Broer: *Rev. Sci. Instrum.* **68**, 2027 (1997)
 17. V.H. Reis, J.B. Fenn: *J. Chem. Phys.* **39**, 3240 (1963)
 18. E.W. Becker, K. Bier: *Z. Naturforsch.* **9a**, 975 (1954)
 19. J. Fernandez de la Mora, B.L. Halpern, J.A. Wilson: *J. Fluid. Mech.* **149**, 217 (1984)
 20. A.-L. Barabasi, H.E. Stanley: *Fractal Concepts in Surface Growth* (Cambridge University Press, Cambridge 1995)
 21. L. Bardotti, P. Jensen, A. Hoareau, M. Treilleux, B. Cabaud, A. Perez, F. Cadete Santos Aires: *Surf. Sci.* **367**, 276 (1996)
 22. P. Melinon, G. Fuchs, B. Cabaud, A. Hoareau, P. Jensen, V. Paillard, M. Treilleux: *J. Phys. I* **3**, 1585 (1993)
 23. K.H. Guenther: *Appl. Opt.* **23**, 3806 (1984)
 24. J. Robertson: *Prog. Solid State Chem.* **21**, 199 (1991)
 25. M. Akagi, H. Nishiguchi, H. Shirakawa: *Synth. Met.* **17**, 557 (1987)
 26. C.E. Bottani, A. Ferrari, A. Li Bassi, P. Milani, P. Piseri: *Europhys. Lett.* **42**, 431 (1998)